# Geometric Distillation for Graph Networks

**Anonymous Author(s)**
Affiliation
Address
email

## Abstract

We study a new paradigm of knowledge transfer in the context of geometric deep learning, which aims at distilling knowledge from a teacher graph neural network (GNN) model trained on a large graph to a student GNN model operating on a smaller graph. To this end, we revisit the connection between thermodynamics and the behavior of GNN, based on which we propose Neural Heat Kernel (NHK) to encapsulate the geometric property of the underlying manifold concerning the architecture of GNN. A natural solution is derived by analysing and aligning NHKs on teacher and student models, dubbed as Geometric Knowledge Distillation. We develop non- and parametric instantiations and demonstrate their efficacy in various experimental settings for knowledge distillation regarding different types of privileged topological information and teacher-student schemes.

## 1 Introduction

Modern graph neural networks (GNNs) [23, 39, 43] have shown remarkable performance in learning representations for structured instances. From the perspective of geometric deep learning [4, 3, 30], much of the achievement of GNNs can be attributed to their successful implementation of the permutation invariance property as *geometric priors* [1] into the architecture design. Nevertheless, in practice, GNNs highly rely on graph topology, as essential input information, to explore the relational knowledge implicit in interactions of instance pairs throughout the entire message passing process, termed as *geometric knowledge* in this paper. As advances in generalized distillation [25, 37] reveal the possibility of encoding input features into model construction, natural questions arise as to:

*Is it possible, and if so, how can we encode graph topology as a special type of 'geometric prior' into a GNN model, such that the model could precisely capture the underlying geometric knowledge even without full graph topology as input?.*

In specific, we are interested in the following *geometric knowledge transfer* problem: a GNN model (with node-specific outputs for node-level prediction [19]) is exposed with a partial graph, which is a subset of the complete graph. Formally speaking, we have notations:

$$\mathcal{G} = \{\mathcal{V}, \mathcal{E}\} \text{ (partial graph)}, \ \tilde{\mathcal{G}} = \{\tilde{\mathcal{V}}, \tilde{\mathcal{E}}\} \text{ (complete graph)}, \ \text{where } \mathcal{V} \subseteq \tilde{\mathcal{V}}, \mathcal{E} \subseteq \{\mathcal{V} \times \mathcal{V}\} \cap \tilde{\mathcal{E}}. \quad (1)$$

Our goal is to transfer or encode geometric knowledge extracted from $\tilde{\mathcal{G}}$ to the target GNN model that is only aware of $\mathcal{G}$. Besides of academic interest, studying this problem is also of much practical value. As a non-exhaustive list of applications: improving efficiency without compromising on effectiveness for coarsened graphs [11, 20, 52], privacy constrained scenarios in social recommenders or federated learning where the complete graph is unavailable [26, 40, 51], promoting concentration on targeted community to bring up economic benefits [44].

[1] Geometric priors originally refer to the geometric principles naturally encoded in deep learning architectures, e.g., translational symmetry for CNNs, permutation invariance for GNNs.

Submitted to 36th Conference on Neural Information Processing Systems (NeurIPS 2022). Do not distribute.

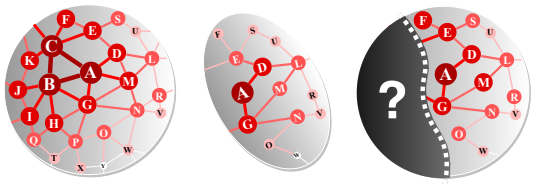


a) Teacher b) Student (before GKD) c) Student (after GKD)

Figure 1: Feature propagation on the underlying manifold $\mathcal{M}$. (a) Teacher: aware of the complete graph topology, and faithfully explore geometric knowledge about the underlying manifold. (b) Student before GKD: only aware of partial graph topology, and estimate biased geometry property. (c) Student after GKD: able to propagate features on the same space as teacher by alignment of neural heat kernels.

Achieving this target is non-trivial for that we need to first answer "what is geometric knowledge and how to translate it into an explicit form", which requires in-depth investigation on the role of graph topology throughout the progressive process of message passing. Therefore, we take a thermodynamic view borrowed from physics and propose a new methodology built upon recent advances revealing the connection between heat diffusion and architectures of GNNs [7, 41, 6]. Specifically, we interpret feature propagation as heat flows on the underlying Riemmanian manifold, whose characteristics (that are dependent on graph topology and the GNN model) pave the way for a principled representation of the latent geometric knowledge.

### 1.1 Our Contributions

**New theoretical perspective for analyzing latent graph geometry.** On top of the well-established connection between heat equation and GNNs, we step further to inspect the implication of heat kernel for existing GNNs, and propose a novel notion of *Neural Heat Kernel* (NHK) with rigorous proof of its existence. Heat kernel intrinsically defines the unique solution to the heat equation and can be a fundamental characterization for the geometric property of the underlying manifold [14, 15]. Likewise, NHK uncovers geometric property of the latent graph manifold for GNNs, and governs how information flows between pairs of instances. It lends us a tractable mathematical tool to understand what geometric knowledge the GNN model has learned or extracted from the graph topology.

**Flexible distillation framework with versatile instantiations.** Based on the insights mentioned above, we treat NHK matrices as representation of the latent geometric knowledge, upon which we build a flexible and principled distillation framework dubbed as *Geometric Knowledge Distillation* (GKD), which aims at encoding and transferring geometric knowledge by aligning latent manifolds behind GNN models as illustrated in Fig. 1. Moreover, we develop non-parametirc and parametric versions of GKD, in terms of different ways to approximate NHK computation. Specifically, the former derives explicit NHKs via assumptions on latent space, and the later learns NHK in a data-driven manner through the lens of variational inference, which will be shown to match two models by minimizing the KL-divergence of their distributions.

**Promising results for geometric knowledge transfer and conventional KD purposes.** We verify the practical efficacy of GKD in terms of different geometric knowledge types (i.e., edge-aware and node-aware ones), and further show its effectiveness for conventional KD purposes (e.g., model compression, self-distillation). We highlight that our methods consistently exceed teacher model and even rival with the oracle model that gives the performance upper bound in principle.

### 1.2 Links to Related Works

**Geometric Deep Learning.** The study of geometric deep learning [4, 30] provides fundamental principles and methodology to generalize deep learning methods to non-Euclidean domains (e.g., graphs and manifolds). From this perspective, architectures for off-the-shelf GNNs [23, 39, 43, 16] have naturally incorporated the geometric prior knowledge for graphs such as *permutation invariance*. Despite their remarkable success, they highly rely on the graph topology. This work extends the idea of geometric deep learning by treating the global graph topology as a special type of prior knowledge, and attempts to encode it into GNNs themselves, such that the trained model would leverage information from the global graph topology even without explicitly taking it as input.

**Graph-Based Knowledge Distillation.** Knowledge distillation (KD) [18, 1] uses the outputs of a teacher model as alternative supervised signals to teach a student model, with various new paradigms including feature-based [33, 50] and relation-based [49] ones. While some prior arts [8, 47, 40, 48, 46] attempted to combine KD and GNNs, i.e., graph-based KD, they are nearly straight-forward adaptations of KD without in-depth investigation on the role of graph topology, also restricted by a

specific choice of GNN architecture or application scenarios, e.g., model compression. In contrast, we first formalize the problem of geometric knowledge transfer, theoretically answer the question "how to represent graph geometric knowledge and encode it into GNN models", and propose geometric distillation approach based on the theoretical results, which is shown to be effective in various settings.

## 2 Preliminaries

We commence with a brief detour to heat equation on Riemannian manifolds, and its connection with modern GNN architectures. Moreover, we bring forth the notion of *heat kernel* to motivate this work.

**Heat Equation on Manifolds.** We are interested in heat equation defined on a smooth $k$-dimensional Riemannian manifold $\mathcal{M}$. Suppose the manifold is associated with a scalar- or vector-valued function $x(u,t) : \mathcal{M} \times [0,\infty) \to \mathbb{R}^d$, quantifying a specific type of signals such as *heat* at a point $u \in \mathcal{M}$ and time $t$. Fourier's law of heat conductivity describes the flow of heat with respect to time and space, via a partial differential equation (PDE) called *heat equation* [5], i.e.,

$$\frac{\partial x(u,t)}{\partial t} = -c\,\Delta x(u,t), \tag{2}$$

where $c > 0$ is the *thermal conductivity* coefficient, and $\Delta$ is the natural *Laplace–Beltrami operator* associated with $\mathcal{M}$. Rewriting $\Delta$ as the functional composition of the *divergence operator* $\nabla^*$ and *gradient operator* $\nabla$, i.e., $\Delta = \nabla^* \circ \nabla$, we can interpret the heat equation as: the variation of temperature within an infinitesimal time interval at a point is equivalent to the divergence between its own temperature and the average temperature on an infinitesimal sphere around it.

**Implications on Graphs.** A spatial discretisation of a continuous manifold yields a graph $\mathcal{G} = \{\mathcal{V}, \mathcal{E}\}$, whose nodes can be thought of as embedded on the base manifold. In fact, the heat equation along with variants thereof (e.g., Schrödinger equation) have found widespread use in modeling graph dynamics [10, 21, 28]. More importantly, it has been recently revealed to be intimately related with the architectures of modern GNNs [41, 7, 6]: suppose $\mathbf{X}(0) = \{x(u,0)\}_{u\in\mathcal{V}} \in \mathbb{R}^{n\times d}$ denotes the initial condition for Eqn. (2) determined by input node features, then solving the heat equation under certain definitions of $\nabla^*$ and $\nabla$ (i.e., definition of $\Delta$) amounts to different architectures of GNNs. For instance:

**Example 1.** [41] Define the discretised counterpart of $\Delta$ as the graph Laplacian matrix $\mathbf{L} = \widetilde{\mathbf{D}}^{-\frac{1}{2}}(\widetilde{\mathbf{D}} - \widetilde{\mathbf{A}})\widetilde{\mathbf{D}}^{-\frac{1}{2}}$. Numerically solving Eqn. (2) using the forward Euler method with step size $\tau = 1$ yields the formulation of Simple Graph Convolution (SGC) [43]

$$\hat{\mathbf{X}}(t) = \left(\tilde{\mathbf{D}}^{-\frac{1}{2}}\tilde{\mathbf{A}}\tilde{\mathbf{D}}^{-\frac{1}{2}}\right)^t \mathbf{X}(0), \quad \hat{\mathbf{Y}} = \sigma\left(\hat{\mathbf{X}}(t)\mathbf{\Theta}\right). \tag{3}$$

**Example 2.** [7] Define the gradient operator $\nabla_{ij}$ as the difference of source and target node features, the divergence operator $\nabla_i^*$ as the sum of features of all edges for the node. Numerically solving Eqn. (2) using the explicit Euler scheme with step size $\tau$ yields the following recursive formulation

$$\hat{\mathbf{X}}(t+\tau) = \tau\left(\mathbf{G} - I\right)\hat{\mathbf{X}}(t) + \hat{\mathbf{X}}(t) \tag{4}$$

where $\mathbf{G}$ is a diffusivity coefficient matrix in place of $c$.

Moreover, stacking a non-linear transformation layer after each step yields the formulation of Graph Convolution Networks (GCN) [23] for Eqn. (3), Graph Attention Networks (GAT) [39] with residual connection for Eqn. (4), and even more GNN architectures by virtue of the flexibility of interpretion for heat equation on graphs.

**Heat Kernels** Intriguingly, it turns out that the initial value problem of heat equation on any manifold $\mathcal{M}$ has a smallest positive fundamental solution depending on the Laplace operator $\Delta$, known as the *heat kernel* [2]. It is denoted as a kernel function $\kappa(x,y,t)$, such that

$$x(u_i,t) = e^{-t\Delta}x(u_i,0) = \int_{\mathcal{M}} \kappa(u_i,u_j,t)x(u_j,0)\mathrm{d}\mu(u_j), \tag{5}$$

where $\mu$ is a non-negative measure associated with $\mathcal{M}$. In physics, the heat kernel $\kappa(x,y,t)$ can be interpreted as a transition density that describes the asymptotic behavior of a natural Brownian

motion on the manifold. Its formulation thus can be treated as *a unique reflection or representation of the geometry of the underlying manifold*. For example, if the manifold is a $k$-dimensional *Euclidean Space* $\mathbb{R}^k$ or a *Hyperbolic Space* $\mathbb{H}^k$, the explicit formula of heat kernel is respectively given by,

$$\kappa(u_i, u_j, t) = \frac{1}{(4\pi t)^{k/2}} \exp\left(-\frac{\rho^2}{4t}\right) \text{ and } \kappa(u_i, u_j, t) = \frac{(-1)^m}{2^m \pi^m} \frac{1}{(4\pi t)^{\frac{1}{2}}} \left(\frac{1}{\sinh \rho} \frac{\partial}{\partial \rho}\right)^m e^{-m^2 t - \frac{\rho^2}{4t}}, \quad (6)$$

where $\rho = d(u_i, u_j)$ denote geodesic distance. Heat kernel has also been adopted for graph-related applications such as community detection [24], graph clustering [45].

# 3 Extending Heat Kernel to GNNs

The starting point of this work is the development of *neural heat kernel*, built upon the previously-mentioned connection of GNNs and heat equation. As will be discussed later, this novel notion lends us a thermodynamic perspective to the intrinsic geometric property of the latent graph manifold embodied in GNNs, and hence paves the way for distilling geometric knowledge.

## 3.1 Neural Heat Kernel

Consider the graph signal $\mathbf{X}(t)$ at time $t$ and node features $\mathbf{H}^{(l)}$ at layer $l$ as interchangeable notions. Consequently, feature propagation using one layer of GNN amounts to heat diffusion on the base manifold $\mathcal{M}$ within a certain time interval $\tau$, leading to the equivalences of $\mathbf{X}(t+\tau)$ and $\mathbf{H}^{(l+1)}$:

$$\mathbf{H}^{(l+1)} = f_\theta(\mathbf{H}^{(l)}, \mathcal{G}), \ \mathbf{X}(t+\tau) = e^{-\tau \Delta(\theta, \mathcal{G})} \mathbf{X}(t), \quad (7)$$

where $f_\theta$ denotes an arbitrary GNN model with parameter $\theta$, and $\Delta(f_\theta, \mathcal{G})$ denotes a generalization of Laplace-Beltrami operator defined over the base manifold $\mathcal{M}$ associated with graph $\mathcal{G}$ and the arbitrary backbone GNN model $f_\theta$.

In light of this connection, we consider a natural generalization of heat kernel for GNNs, termed as *neural heat kernel (NHK)* to highlight its difference with heat kernel in the thermodynamic context. In particular, a *single-layer* NHK is defined as a positive definite symmetric kernel function denoted as $\kappa_\theta^{(l)}(v_i, v_j)$, where the sub-script $\theta$ implies that it is associated with the architecture and parameters of the backbone GNN, and the super-script $(l)$ implies that it is specific to each layer, analogous to the role of continuous time $t$ in Eqn. (5).

**Theorem 1.** ***(Existence of Single-Layer NHK)*** *Suppose two expressions in Eqn. (7) are equivalent, then for any graph $\mathcal{G}$ and GNN model $f_\theta$, there exist a unique single-layer NHK function $\kappa_\theta^{(l)}(\cdot)$ such that for any node $v_i \in \mathcal{V}$ and $l > 0$,*

$$\mathbf{h}_i^{(l)} = \sum_{v_j \in \mathcal{V}} \kappa_\theta^{(l)}(v_i, v_j) \cdot \mathbf{h}_j^{(l-1)} \mu(v_j) \quad (8)$$

*where $\mathbf{h}_i^{(l)} \in \mathbb{R}^d$ denotes the feature of node $v_i$ at $l$-th layer, and $\mu$ is a measure over vertices specified as the inverse of node degree $1/d_i$.*

To push further, we can generalize NHK across multiple layers of GNN, termed as a *cross-layer NHK* $\kappa_\theta(v_i, v_j, l \mapsto l+k)$ (e.g., from $l$-th layer to $(l+k)$-th layer of GNN). Its existence could be induced recursively by the *semi-group identity property* of NHK concerning consecutive GNN layers.

**Theorem 2.** ***(Semigroup Identity Property of NHK)*** *The NHK satisfies the semigroup identity property: $\forall v_i, v_j \in \mathcal{V}$ and $l > 0$, there exists a cross-layer NHK across two consecutive layers*

$$\kappa_\theta(v_i, v_j, l \mapsto l+2) = \sum_{v_k \in \mathcal{V}} \kappa_\theta^{(l+1)}(v_i, v_k) \kappa_\theta^{(l+2)}(v_k, v_j) d\mu(v_k) \quad (9)$$

This theorem indicates that stacks of multiple GNN layers also constitute a valid kernel, i.e.,

$$\mathbf{h}_i^{(l+k)} = \sum_{v_j \in \mathcal{V}} \kappa_\theta(v_i, v_j, l \mapsto l+k) \cdot \mathbf{h}_j^{(l)} \mu(v_j). \quad (10)$$

Analogous to heat kernel as an unique characterization of the underlying space, NHK characterizes the geometric property of the latent graph manifold for GNNs. Additionally, NHK is dependent on GNN models through the definition of the associated Laplace-Beltrami operator $\Delta(f_\theta, \mathcal{G})$, inheriting the expressiveness of neural networks and varying through the course of training. Intuitively, NHK can be thought of as a model-driven encoding for topological information, encapsulating the geometric knowledge learned by GNNs into a tractable functional form.

### 3.2 Application in Geometric Distillation

Consider the problem of distilling geometric knowledge, which involves an intelligent teacher model $f_{\theta^*}$, which is exposed to and pre-trained over the (relatively) *complete graph* $\tilde{\mathcal{G}} = (\tilde{\mathcal{V}}, \tilde{\mathcal{E}})$, and a student model $f_\theta$ that is exposed to the partial graph $\mathcal{G} = (\mathcal{V}, \mathcal{E})$, where $\mathcal{V} \subseteq \tilde{\mathcal{V}}$ and $\mathcal{E} \subseteq \{\mathcal{V} \times \mathcal{V}\} \cap \tilde{\mathcal{E}}$. Our target is to train a student model (with the help of teacher model) that operates on $\mathcal{G}$ to be as competitive as models operating on $\tilde{\mathcal{G}}$ during inference. Since $\mathcal{G}$ is a sub-graph of $\tilde{\mathcal{G}}$, they should lie in the *same space* (i.e., latent manifold) governed by the underlying mechanism of data generation, and hence we expect student and teacher models to capture the *same geometric property* of this shared space. This leads to the principle of *Geometric Knowledge Distillation* (GKD): transfer the geometric knowledge of the intelligent teacher to the student such that the student can propagate features as if it is aware of the complete graph topology (see the example in Fig. 1).

To this end, we resort to *NHK matrices* on the teacher (resp. student) model over the complete (resp. partial) graph as instantiations of their geometric knowledge, denoted as

$$\text{(Teacher)} \quad \mathbf{K}_{\theta^*}(\tilde{\mathcal{G}}, l \mapsto l+k) = \{\kappa_{\theta^*}(v_i, v_j, l \mapsto l+k)\}_{|\tilde{\mathcal{V}}| \times |\tilde{\mathcal{V}}|},$$
$$\text{(Student)} \quad \mathbf{K}_{\theta}(\mathcal{G}, l \mapsto l+k) = \{\kappa_{\theta}(v_i, v_j, l \mapsto l+k)\}_{|\mathcal{V}| \times |\mathcal{V}|},$$

written compactly as $\mathbf{K}^{(l+1)}(\mathcal{G})$ when $k = 1$. The NHK matrix is a positive semi-definite symmetric matrix, and alike $\kappa$, is dependent on the GNN model $f_\theta$ and graph $\mathcal{G}$. Denote $\mathbf{K}^{(l)}_{\theta^*,\mathcal{V}}(\tilde{\mathcal{G}}) \in \mathbb{R}^{|\mathcal{V}| \times |\mathcal{V}|}$ as the sub-matrix of $\mathbf{K}^{(l)}_{\theta^*}(\tilde{\mathcal{G}})$ with row and column indices in $\mathcal{V}$. The distillation loss for GKD is

$$\mathcal{L}_{dis}(\mathbf{K}_{\theta^*,\mathcal{V}}, \mathbf{K}_\theta, l \mapsto l+k) = \mathrm{d}(\mathbf{K}_{\theta^*,\mathcal{V}}(\tilde{\mathcal{G}}, l \mapsto l+k), \mathbf{K}_\theta(\mathcal{G}, l \mapsto l+k)), \tag{11}$$

where $\mathrm{d}(\cdot, \cdot)$ is a similarity measure, for which we choose Frobenius distance as implementation, i.e.,

$$\mathrm{d}(\mathbf{K}_{\theta^*,\mathcal{V}}, \mathbf{K}_\theta) = \|(\mathbf{K}_{\theta^*,\mathcal{V}} - \mathbf{K}_\theta) \odot \mathbf{W}\|_{\mathrm{F}}^2, \quad \mathbf{W}_{v_i,v_j} = \begin{cases} 1 & \text{if} \quad (v_i, v_j) \in \mathcal{E} \\ \delta & \text{if} \quad (v_i, v_j) \notin \mathcal{E}. \end{cases} \tag{12}$$

where $\mathbf{W} \in \mathbb{R}^{|\mathcal{V}| \times |\mathcal{V}|}$ is a weighting matrix to trade-off distillation loss with respect to different node pairs depending on their connectivity. For $k = 1$, the loss can be re-written as $\mathcal{L}^{(l+1)}_{dis}(\mathbf{K}_{\theta^*,\mathcal{V}}, \mathbf{K}_\theta)$. Note that one can also specify different $k$ for teacher and student models in Eqn. (11) in case when the teacher model is deeper. We also study the impact of different similarity measures in Appendix F.1.

## 4 Instantiations for Geometric Knowledge Distillation

Unfortunately, deriving explicit formulas for NHKs is prohibitively challenging due to introduction of non-linearity. To circumvent it, we propose two types of instantiations for GKD, i.e., non-parametric and parametric. The former considers explicit NHKs by making assumptions on the underlying space, and the latter resorts to variational inference techniques to learn NHK in a data-driven manner.

### 4.1 Non-Parametric Geometric Distillation

**Deterministic Kernel.** One instantiation of NHK is a *Gauss-Weierstrass kernel* in the form of Eqn. (6), by assuming the underlying space is a Euclidean space. Since the distillation loss in Eqn. (11) is a homogeneous function, we can remove its scaling factor and define NHK as

$$\text{(Gauss-Weierstrass NHK)} \quad \kappa_\theta(v_i, v_j, l \mapsto l+k) \triangleq \exp\left(-\frac{\|\mathbf{h}_i^{(l)} - \mathbf{h}_j^{(l)}\|_2^2}{4T}\right), \tag{13}$$

where $T$ denotes the estimation of the accumulated time interval. Alternatively, we can use *Sigmoid kernel* and define non-parametric NHK as:

$$\text{(Sigmoid NHK)} \quad \kappa_\theta(v_i, v_j, l \mapsto l+k) \triangleq \tanh\left(a \, \langle \mathbf{h}_i^{(l)}, \mathbf{h}_j^{(l)} \rangle + b\right), \tag{14}$$

where $a, b$ are positive constants depending on $l$ and $k$. It is a natural and intuitive choice as similarity measurement and empirically found as-well effective, albeit does not correspond to any named manifold to our knowledge.

**Randomized Kernel.** We can also define *Randomized kernel* based on the following theorem.

**Theorem 3.** ***(Expansion of NHK)*** *Let $\{\varphi_{k'}\}_{k'=0}^{\infty}$ be orthonormal basis of eigenfunctions of $-\Delta(f_\theta, \mathcal{G})$ with eigenvalues $0 < \lambda_0 \leq \lambda_1 \leq \lambda_2 \leq \ldots$, NHK allows the expansion:*

$$\kappa_\theta(v_i, v_j, l \mapsto l+k) = \sum_{k'=0}^{\infty} e^{-\lambda_{k'}T} \varphi_{k'}(v_i)^\top \varphi_{k'}(v_j). \tag{15}$$

Based on this result, we resort to the approximation of NHK by defining a randomized kernel in a similar form as Eqn. (15), leading to the following formulation of randomized NHK:

$$\text{(Randomized NHK)} \quad \kappa_\theta(v_i, v_j, l \mapsto l+k) \triangleq \frac{1}{m} \sum_{k'=0}^{m} e^{-\lambda_{k'}T} \left[\sigma\left(\boldsymbol{W}_{k'}\mathbf{h}_i\right)^\top \sigma\left(\boldsymbol{W}_{k'}\mathbf{h}_j\right)\right], \tag{16}$$

where $\sigma\left(\boldsymbol{W}_{k'}\mathbf{h}_i\right)$ is used to proximate $\varphi_{k'}\left(v_i\right)$, $\boldsymbol{W}_{k'} = \left[\boldsymbol{\phi}_{1,k'}, \boldsymbol{\phi}_{2,k'}, \cdots, \boldsymbol{\phi}_{s,k'}\right]^\top$ is a transformation matrix, $\boldsymbol{\phi} \sim \mathcal{N}\left(\mathbf{0}, \boldsymbol{I}_d\right)$ is a $d$-dimensional random variable from Gaussian distribution. In fact, under certain choice of activation function $\sigma$, Eqn. (16) could approximate a diversity of kernels [32, 9]. This design essentially enforces the alignment of teacher and student for arbitrary underlying manifold.

**Training Scheme.** We follow the standard training paradigm in KD literature [18, 13]: the teacher is pre-trained by a supervised prediction loss involving all labeled nodes in $\tilde{\mathcal{V}}$. After teacher is well-trained, we fix $\theta^*$ and train the student model according to

$$\theta = \arg\min_\theta \mathcal{L}_{pre}(\hat{\mathbf{Y}}_\theta, \mathbf{Y}) + \frac{\alpha}{L} \sum_{l=1}^{L} \mathcal{L}_{dis}^{(l)}(\mathbf{K}_{\theta^*,\mathcal{V}}, \mathbf{K}_\theta), \tag{17}$$

where $\mathbf{Y}$ denotes ground-truth labels of labeled nodes in $\mathcal{V}$, and $\hat{\mathbf{Y}}_\theta$ denotes the predictions of student model $f_\theta$ on $\mathcal{G}$, $\mathcal{L}_{dis}$ is the distillation loss defined by Eqn. (11), $L$ denotes the total number of layers.

### 4.2 Parametric Geometric Distillation

Inheriting the similar spirit of auto-encoding Bayes [22], we introduce a *variational inverse-NHK* that is independently parameterized, denoted as $\kappa_\phi^\dagger$, whose existence is guaranteed by the invertibility of NHK matrices. Together with $\kappa_\theta$, they define a symmetric form characterizing feature propagation:

$$\text{(Forward)} \quad \mathbf{h}_i^{(l+k)} = \sum_{v_j \in \mathcal{V}} \kappa_\theta(v_i, v_j, l \mapsto l+k) \cdot \mathbf{h}_j^{(l)} \mu(v_j), \tag{18}$$

$$\text{(Backward)} \quad \mathbf{h}_i^{(l)} = \sum_{v_j \in \mathcal{V}} \kappa_\phi^\dagger(v_i, v_j, l+k \mapsto l) \cdot \mathbf{h}_j^{(l+k)} \mu(v_j). \tag{19}$$

In practice, we follow existing kernel learning approaches [42] and use deep architectures to parameterize the variational inverse-NHK as

$$\kappa_\phi^\dagger(v_i, v_j, l+k \mapsto l) = g_\phi(\mathbf{h}_i^{(l+k)})^\top g_\phi(\mathbf{h}_j^{(l+k)}), \tag{20}$$

where $g_\phi : \mathbb{R}^d \to \mathbb{R}^s$ is the associated learnable non-linear mapping. Given a pre-trained teacher model, distilling geometric knowledge boils down to 1) establishing equivalence of Eqn. (18) and Eqn. (19), and 2) matching pseudo-inverse NHK matrices for teacher and student models (respectively denoted as $\mathbf{K}_{\theta^*,\mathcal{V}}^\dagger$ and $\mathbf{K}_\theta^\dagger$ with clear meanings), leading to the training scheme as follows.

**Training Scheme.** Based on Eqn. (19), we can define a *reconstruction loss* with respect to the teacher model (similar applies to the student model) as

$$\mathcal{L}_{rec}(\mathbf{H}_t^{(l+k)}, \mathbf{H}_t^{(l)}) = \|\mathbf{K}_{\theta^*}^\dagger \tilde{\mathbf{D}}^{-1} \mathbf{H}_t^{(l+k)} - \mathbf{H}_t^{(l)}\|_F^2, \tag{21}$$

where $\tilde{\mathbf{D}}$ denotes the degree matrix over $\tilde{\mathbf{G}}$. Then, minimizing the reconstruction loss with fixed GNN model parameter $\theta$ amounts to optimizing the variational parameter $\phi$, and minimizing prediction and distillation losses given fixed $\phi$ amounts to optimizing the student model parameter $\theta$:

$$\phi \leftarrow \arg\min_\phi \quad \beta \mathcal{L}_{rec}\left(\mathbf{H}_t^{(l+k)}, \mathbf{H}_t^{(l)}\right) + (1-\beta)\mathcal{L}_{rec}\left(\mathbf{H}^{(l+k)}, \mathbf{H}^{(l)}\right), \tag{22}$$

$$\theta \leftarrow \arg\min_\theta \quad \mathcal{L}_{pre}\left(\hat{\mathbf{Y}}_\theta, \mathbf{Y}\right) + \alpha \mathcal{L}_{dis}\left(\mathbf{K}_{\theta^*,\mathcal{V}}^\dagger, \mathbf{K}_{\theta^*,\mathcal{V}}^\dagger, l+k \mapsto l\right). \tag{23}$$

Applying two steps iteratively adds up to an EM-like algorithm for training the student model. In practice, we set $l+k$ as the last layer, and $l$ as the first layer.

**Justification.** We justify parametric GKD from a variational inference perspective. From Eqn. (18), the forward GNN model $f_\theta$ defines a model distribution $p_\theta(\mathbf{H}^{(l)}, \mathbf{H}^{(l+k)}, \mathbf{K}) = p_\theta(\mathbf{H}^{(l)}) p_\theta(\mathbf{K}|\mathbf{H}^{(l)}) p_\theta(\mathbf{H}^{(l+k)}|\mathbf{K}, \mathbf{H}^{(l)})$, where $p_\theta(\mathbf{K}|\mathbf{H}^{(l)})$ is intractable, hindering the proceeding distillation. In this light, the variational inverse-NHK model $\kappa_\phi^\dagger$ is proposed with a variational distribution $q_\phi(\mathbf{H}^{(l)}, \mathbf{H}^{(l+k)}, \mathbf{K}) = q_\phi(\mathbf{H}^{(l+k)}) q_\phi(\mathbf{K}|\mathbf{H}^{(l+k)}) q_\phi(\mathbf{H}^{(l)}|\mathbf{H}^{(l+k)}, \mathbf{K})$, which has a tractable posterior $q_\phi(\mathbf{K}|\mathbf{H}^{(l+k)})$. Now, we justify our training scheme with iterative optimization for Eqn. (22) and (23) by the following proposition and refer the reader to Appendix D for detailed reasoning.

**Proposition 1.** *The optimization in Eqn. (22) and (23) essentially minimizes the following Kullback–Leibler (KL) divergence,*

$$\min_{\theta,\phi} \mathcal{D}_{kl}\left(q_\phi(\mathbf{K}, \mathbf{H}^{(l)}, \mathbf{H}^{(l+k)}) \parallel p_\theta(\mathbf{K}, \mathbf{H}^{(l)}, \mathbf{H}^{(l+k)})\right), \tag{24}$$

*and hence attempts to establish equivalence between two latent variable models $p_\theta$ and $q_\phi$.*

# 5 Experiments

We conduct experiments to validate the efficacy of our method on graph-structured data in terms of various types of privileged geometric knowledge, combinations of teacher-student GNN architectures and potential application scenarios. We use three benchmark datasets Cora [27], Citeseer [35], Pubmed [31], and two larger datasets, i.e., OGBN-Proteins and OGBN-Arxiv [19], for node classification tasks. More details are given in Appendix E.

**Implementation and Competitors** We consider the following variants of the proposed GKD. 1) *GKD-G*: non-parametric Gaussian NHK; 2) *GKD-S*: non-parametric Sigmoid NHK; 3) *GKD-R*: randomized NHK; 3) *VGKD*: parametric variational NHK. We choose KD methods that is representative in its own category for comparison, including *KD* [18], *FitNets* [33],*FSP* [49],*TinyGNN* [46],*LSP* [48]. Implementation details and descriptions of baselines are deferred to Appendix. We also report the performances of teacher and student model trained with the standard classification loss, short as *Teacher* and *Student*. The teacher model is trained using the complete graph $\tilde{\mathcal{G}}$, and, to calibrate with all other methods, tested using the partial graph $\mathcal{G}$. Besides, we consider an *Oracle* model which is both trained and tested on $\tilde{\mathcal{G}}$, which naturally takes an advantaged place given more information during inference. Since our method is compatible with the vanilla KD paradigm [18], we report the performance delivered by their combinations (i.e., GKD+KD and VGKD+KD).

**Experiment Settings** We investigate on various experimental settings according to different types of privileged geometric knowledge. In the case of *edge-aware geometric knowledge*, the teacher model has access to additional edge information, i.e., $\mathcal{E} \subset \tilde{\mathcal{E}}$ and $\mathcal{V} = \tilde{\mathcal{V}}$. In the case of *node-aware geometric knowledge*, the teacher model has access to additional node information, i.e., $\mathcal{V} \subset \tilde{\mathcal{V}}$ and $\mathcal{E} = \tilde{\mathcal{E}} \cap \{\mathcal{V} \times \mathcal{V}\}$. We also consider other conventional or novel settings including model compression, self-distillation, teaching MLP, which will be illustrated in detail. The backbone $f_\theta$ is set as 3-layer GCN [23] for both student and teacher models, unless otherwise stated. All the experiments are repeated five times with random initialization.

## 5.1 Edge-Aware Geometric Knowledge

We report results for the edge-aware geometric knowledge setting, where the teacher model has access to auxiliary edges. To quantify the privileged information, we set the quantity $(|\tilde{\mathcal{E}}| - |\mathcal{E}|)/|\tilde{\mathcal{E}}|$, called *privileged information ratio* (PIR), as $0.5$. As shown in Tab. 1, all variants of GKD outperform other KD baselines by a large margin on both datasets, and significantly exceeds both Student and Teacher models. Further, GKD and its variants rival, if not surpass, the Oracle model. In other words, the student model trained using GKD could use far less graph topological information to achieve very close performance to competitors that are aware of the full graph topology during inference. This implies that our GKD framework could indeed effectively transfer topological information.

With regard to comparison among the variants of GKD, the parametric VGKD performs better than its non-parametric counterparts in most cases, and GKD-R is the most effective non-parametric method in general. Despite these results, GKD-G and GKD-S are also effective while being simpler and more

| | Cora | CiteSeer | PubMed |
|---|---|---|---|
| Oracle | $88.63 \pm 0.48$ | $73.64 \pm 0.48$ | $87.16 \pm 0.19$ |
| Teacher | $84.61 \pm 0.37$ | $70.88 \pm 0.62$ | $84.42 \pm 0.52$ |
| Student | $83.84 \pm 1.32$ | $69.94 \pm 0.76$ | $85.35 \pm 0.43$ |
| KD | $84.84 \pm 1.19$ | $70.04 \pm 0.37$ | $85.58 \pm 0.32$ |
| FitNets | $83.72 \pm 1.45$ | $69.99 \pm 0.56$ | $85.66 \pm 0.27$ |
| FSP | $83.55 \pm 2.19$ | $71.43 \pm 1.26$ | $85.46 \pm 0.34$ |
| TinyGNN | $83.92 \pm 0.53$ | $71.62 \pm 0.31$ | $83.92 \pm 0.53$ |
| LSP | $83.99 \pm 1.39$ | $70.23 \pm 0.79$ | $85.37 \pm 0.49$ |
| GKD-G | $87.68 \pm 1.07$ | $73.04 \pm 0.70$ | $85.74 \pm 0.38$ |
| GKD-S | $88.01 \pm 0.79$ | $72.46 \pm 0.52$ | $85.94 \pm 0.43$ |
| GKD-R | $\mathbf{88.48 \pm 0.59}$ | $72.97 \pm 0.53$ | $86.19 \pm 0.55$ |
| VGKD | $88.41 \pm 0.62$ | $\mathbf{73.12 \pm 0.58}$ | $\mathbf{86.41 \pm 0.24}$ |
| GKD+KD | $88.95 \pm 0.30$ | $73.21 \pm 0.53$ | $86.29 \pm 0.28$ |
| VGKD+KD | $\mathbf{89.09 \pm 0.40}$ | $\mathbf{73.45 \pm 0.48}$ | $\mathbf{86.48 \pm 0.52}$ |

Table 1: Results of node classification accuracy for the edge-aware knowledge setting.

| | Cora | CiteSeer | PubMed |
|---|---|---|---|
| Oracle | $88.63 \pm 0.48$ | $73.64 \pm 0.48$ | $87.16 \pm 0.19$ |
| Teacher | $87.27 \pm 0.51$ | $72.92 \pm 0.90$ | $85.98 \pm 0.23$ |
| Student | $84.84 \pm 1.61$ | $70.32 \pm 1.12$ | $84.74 \pm 0.27$ |
| KD | $86.71 \pm 0.77$ | $71.96 \pm 1.10$ | $85.55 \pm 0.45$ |
| FitNets | $86.09 \pm 1.12$ | $72.00 \pm 0.78$ | $85.78 \pm 0.26$ |
| FSP | $85.85 \pm 1.66$ | $70.92 \pm 1.46$ | $85.20 \pm 0.45$ |
| TinyGNN | $86.13 \pm 0.52$ | $70.84 \pm 0.73$ | $84.12 \pm 0.51$ |
| LSP | $85.67 \pm 1.22$ | $70.66 \pm 1.01$ | $85.71 \pm 0.50$ |
| GKD-G | $88.66 \pm 0.85$ | $73.18 \pm 0.88$ | $86.07 \pm 0.45$ |
| GKD-S | $88.54 \pm 0.52$ | $72.85 \pm 0.57$ | $86.10 \pm 0.42$ |
| GKD-R | $88.98 \pm 0.39$ | $72.80 \pm 0.22$ | $\mathbf{86.16 \pm 0.33}$ |
| VGKD | $\mathbf{89.15 \pm 0.45}$ | $\mathbf{73.33 \pm 0.36}$ | $86.09 \pm 0.54$ |
| GKD+KD | $89.10 \pm 0.44$ | $72.94 \pm 0.80$ | $\mathbf{86.24 \pm 0.26}$ |
| VGKD+KD | $\mathbf{89.23 \pm 0.61}$ | $\mathbf{73.41 \pm 0.60}$ | $86.20 \pm 0.36$ |

Table 2: Results of node classification accuracy for the node-aware setting.

| Dataset | Setting | Oracle | Teacher | Student | KD | GKD | VGKD |
|---|---|---|---|---|---|---|---|
| OGBN-Proteins | Edge-Aware | $72.39 \pm 0.52$ | $70.89 \pm 0.43$ | $67.75 \pm 0.21$ | $69.51 \pm 0.36$ | $71.84 \pm 0.32$ | $\mathbf{72.18 \pm 0.34}$ |
| | Node-Aware | $72.39 \pm 0.52$ | $71.22 \pm 0.62$ | $68.90 \pm 0.42$ | $70.23 \pm 0.32$ | $71.92 \pm 0.25$ | $\mathbf{71.99 \pm 0.44}$ |
| OGBN-Arxiv | Edge-Aware | $71.46 \pm 0.41$ | $67.96 \pm 0.78$ | $66.41 \pm 0.45$ | $68.63 \pm 1.21$ | $70.90 \pm 0.80$ | $\mathbf{71.38 \pm 1.01}$ |
| | Node-Aware | $71.46 \pm 0.41$ | $69.35 \pm 0.72$ | $67.49 \pm 0.65$ | $68.86 \pm 0.66$ | $\mathbf{71.31 \pm 0.83}$ | $71.27 \pm 0.70$ |

Table 3: Results of ROC-AUC on OGBN-Proteins dataset, and accuracy on OGBN-Arxiv dataset.

easy-to-implement. We presume that the performance variation of different GKD realizations stem from the different geometric property governed by the feature of datasets. Thus, it is useful to choose a proper implementation of GKD that is suitable for the application.

### 5.2 Node-Aware Geometric Knowledge

We further investigate on the node-aware geometric knowledge setting where the teacher model has access to more labeled nodes and their relations with the rest nodes. We set the PIR w.r.t. labeled nodes, defined as $(|\tilde{\mathcal{V}}_{train}| - |\mathcal{V}_{train}|)/|\tilde{\mathcal{V}}_{train}|$, to $0.5$. A unique challenge of this setting compared to the edge-ware counterpart is that, apart from graph topological information, the student model has less labeled training samples, putting it into disadvantage. As we can see from Tab. 2, The proposed GKD and its variants again consistently outperform KD baselines throughout all the cases, surpasses both Student and Teacher models, and are even as competitive as Oracle.

### 5.3 Results on Larger Datasets

Table 3 presents results on two large graphs, i.e., OGBN-Proteins and OGBN-Arxiv. We follow the data split in original paper [19], and use the same PIR setting as citation networks, and choose the best variant of GKD to report in the table. As shown in the table, again, we found our methods consistently outperform Teacher and Student models, and are close to the performance of the Oracle model, which suggests the effectiveness of GKD in large graphs.

### 5.4 Performance Variation with Privileged Ratio

The results with respect to varying privileged (edge-aware and node-ware) information ratio are given respectively in Fig. 2 and Fig. 3. The performance of Oracle model is invariant as it is trained and tested on the same (complete) graph. In general, for Teacher model, Student model, and vanilla KD, their performance drops dramatically with increasing PIR quantifying the information loss, with vanilla KD's performance lie in-between. In contrast, our method is significantly more robust, only showing slight performance deterioration, exceeding the Teacher model, and approaching the Oracle model. Besides, we find an interesting phenomenon that in the edge-aware setting on Pubmed dataset, the performance of Teacher model is the worst. This is reasonable since the Teacher is trained using fully observed graph, and may perform poorly once the graph topology, which it relies on for accurate results, becomes incomplete at test time.

### 5.5 Other Settings

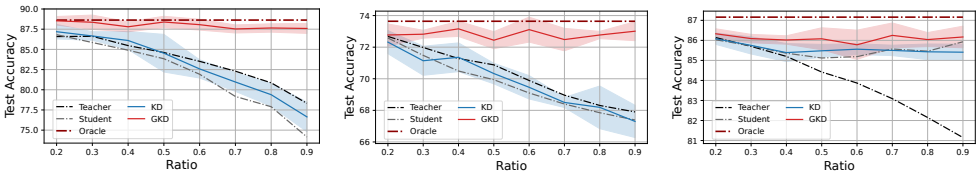


(a) Cora (b) Citeseer (c) Pubmed

Figure 2: Performance variation with increasing PIR for the edge-aware knowledge setting.

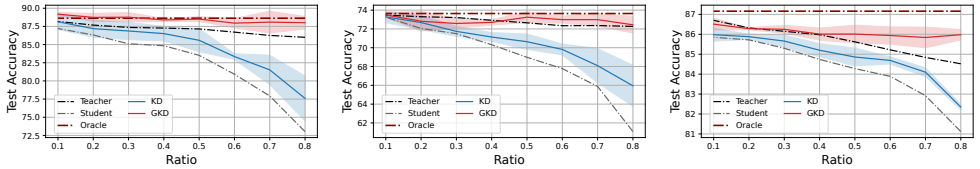


(a) Cora (b) Citeseer (c) Pubmed

Figure 3: Performance variation with increasing PIR for the node-aware knowledge setting.

| Setting | Teacher | Student | KD | GKD |
|---|---|---|---|---|
| Compression | GCN-64 $88.76 \pm 0.34$ | SGC $85.93 \pm 0.17$ | SGC $86.32 \pm 0.32$ | SGC $87.15 \pm 0.85$ |
| | | GCN-8 $84.52 \pm 1.34$ | GCN-8 $87.50 \pm 1.04$ | GCN-8 $88.30 \pm 0.46$ |
| | | GCN-16 $87.24 \pm 0.43$ | GCN-16 $88.09 \pm 0.79$ | GCN-16 $88.62 \pm 0.50$ |
| Self-Distil | GCN-32 $88.63 \pm 0.48$ | | GCN-32 $88.98 \pm 0.34$ | GCN-32 $89.23 \pm 0.52$ |
| | GCN-16 $87.24 \pm 0.43$ | | GCN-16 $87.62 \pm 0.52$ | GCN-16 $88.56 \pm 0.40$ |
| Teach MLP | GCN-32 $88.63 \pm 0.48^1$ $76.75 \pm 2.81^2$ | MLP-32 $70.69 \pm 0.57$ | MLP-32 $72.61 \pm 1.16$ | MLP-32 $88.71 \pm 0.58$ |
| | GCN-16 $87.24 \pm 0.43^1$ $73.21 \pm 5.26^2$ | MLP-16 $68.39 \pm 0.87$ | MLP-16 $71.91 \pm 0.89$ | MLP-16 $87.74 \pm 0.32$ |

[1] Using (resp., [2] Not using) graph at test time.

Table 4: Node classification accuracy on Cora in settings including: 1) model compression; 2) self-distillation; 3) teaching MLP.

**Model Compression** We report the performance of GKD in the conventional model compression setting [18] where the teacher and student are different-sized GNN models. In this setting, we train and test both teacher and student models on the complete graph. We use GCN as the backbone for teacher with a relatively large hidden size 64, and use SGC or GCN (with hidden size 8 and 16) as the student model. We report the best result among all variants of GKD. As shown in the first section of Tab. 4, our method achieves notable improvements over the student model, rendering it as a useful KD approach for model compression.

**Self-Distillation** We further report results for the setting of *self-distillation* [12, 29], which is a special case of KD when the teacher's and student's architectures are identical, often used for refining their own performance. The results as shown in Tab. 4 validate that GKD could also be used to effectively boost GNN's own performance.

**GNNs Teach MLPs** Finally, we study a special setting where any instance relation is unavailable at test time, i.e., $\mathcal{E} = \emptyset$, and examine whether our method could compress the geometric knowledge in this setting when GNN degrades to MLP. The results are shown in Tab. 4. Notably, the performance of conventional GNN model degrades dramatically when the topological information is not available at the test time, while our method turns out to still effective. It again verifies that our method could compress the geometric knowledge into the GNN, and also echoes recent advances in the domain of computer vision, which suggest that MLP could achieve competitive performance with CNN [36].

## 6 Conclusion

This paper formalizes the problem of graph topological knowledge transfer for GNNs. We investigate on the implication of heat kernel in GNNs and propose the novel notion of neural heat kernel. We leverage it to characterize the geometric property of the underlying manifold for graphs, and propose the framework of geometric knowledge distillation to transfer geometric knowledge from a teacher GNN model to a student GNN. Experimental results validate the effectiveness of our approach in various practical settings. The source code will be made public available.

# References


[1] Jimmy Ba and Rich Caruana. Do deep nets really need to be deep? *NeurIPS*, 27, 2014.

[2] Nicole Berline, Ezra Getzler, and Michele Vergne. *Heat kernels and Dirac operators*. Springer Science & Business Media, 2003.

[3] Michael M Bronstein, Joan Bruna, Taco Cohen, and Petar Veličković. Geometric deep learning: Grids, groups, graphs, geodesics, and gauges. *arXiv preprint arXiv:2104.13478*, 2021.

[4] Michael M Bronstein, Joan Bruna, Yann LeCun, Arthur Szlam, and Pierre Vandergheynst. Geometric deep learning: going beyond euclidean data. *IEEE Signal Processing Magazine*, 2017.

[5] John Rozier Cannon. *The one-dimensional heat equation*. Number 23. Cambridge University Press, 1984.

[6] Benjamin Chamberlain, James Rowbottom, Davide Eynard, Francesco Di Giovanni, Xiaowen Dong, and Michael Bronstein. Beltrami flow and neural diffusion on graphs. *NeurIPS*, 2021.

[7] Benjamin Paul Chamberlain, James Rowbottom, Maria Gorinova, Stefan Webb, Emanuele Rossi, and Michael M Bronstein. Grand: Graph neural diffusion. *ICML*, 2021.

[8] Yuzhao Chen, Yatao Bian, Xi Xiao, Yu Rong, Tingyang Xu, and Junzhou Huang. On self-distilling graph neural network. *arXiv preprint arXiv:2011.02255*, 2020.

[9] Youngmin Cho and Lawrence Saul. Kernel methods for deep learning. *NeurIPS*, 22:342–350, 2009.

[10] Fan RK Chung and Fan Chung Graham. *Spectral graph theory*. Number 92. American Mathematical Soc., 1997.

[11] Matthew Fahrbach, Gramoz Goranci, Richard Peng, Sushant Sachdeva, and Chi Wang. Faster graph embeddings via coarsening. In *ICML*, 2020.

[12] Tommaso Furlanello, Zachary Lipton, Michael Tschannen, Laurent Itti, and Anima Anandkumar. Born again neural networks. In *International Conference on Machine Learning*, pages 1607–1616. PMLR, 2018.

[13] Jianping Gou, Baosheng Yu, Stephen J Maybank, and Dacheng Tao. Knowledge distillation: A survey. *International Journal of Computer Vision*, 129(6):1789–1819, 2021.

[14] Alexander Grigoryan. *Heat kernel and analysis on manifolds*, volume 47. American Mathematical Soc., 2009.

[15] Alexander Grigor'yan. Estimates of heat kernels on riemannian manifolds. *London Math. Soc. Lecture Note Ser*, 273:140–225, 1999.

[16] William L Hamilton, Rex Ying, and Jure Leskovec. Inductive representation learning on large graphs. In *NeurIPS*, pages 1025–1035, 2017.

[17] Byeongho Heo, Jeesoo Kim, Sangdoo Yun, Hyojin Park, Nojun Kwak, and Jin Young Choi. A comprehensive overhaul of feature distillation. In *ICCV*, pages 1921–1930, 2019.

[18] Geoffrey Hinton, Oriol Vinyals, and Jeff Dean. Distilling the knowledge in a neural network. *arXiv preprint arXiv:1503.02531*, 2015.

[19] Weihua Hu, Matthias Fey, Marinka Zitnik, Yuxiao Dong, Hongyu Ren, Bowen Liu, Michele Catasta, and Jure Leskovec. Open graph benchmark: Datasets for machine learning on graphs. *NeurIPS*, 33:22118–22133, 2020.

[20] Yu Jin, Andreas Loukas, and Joseph JaJa. Graph coarsening with preserved spectral properties. In *AISTATS*, 2020.

[21] Matthias Keller and Daniel Lenz. Unbounded laplacians on graphs: basic spectral properties and the heat equation. *Mathematical Modelling of Natural Phenomena*, 5(4):198–224, 2010.

[22] Diederik P. Kingma and Max Welling. Auto-encoding variational bayes. In *International Conference on Learning Representations*, 2014.

[23] Thomas N Kipf and Max Welling. Semi-supervised classification with graph convolutional networks. *arXiv preprint arXiv:1609.02907*, 2016.

[24] Kyle Kloster and David F Gleich. Heat kernel based community detection. In *KDD*, pages 1386–1395, 2014.

[25] David Lopez-Paz, Léon Bottou, Bernhard Schölkopf, and Vladimir Vapnik. Unifying distillation and privileged information. *ICLR*, 2016.

[26] Hao Ma, Dengyong Zhou, Chao Liu, Michael R. Lyu, and Irwin King. Recommender systems with social regularization. In *International Conference on Web Search and Web Data Mining*, pages 287–296, 2011.

[27] Andrew Kachites McCallum, Kamal Nigam, Jason Rennie, and Kristie Seymore. Automating the construction of internet portals with machine learning. *Information Retrieval*, 2000.

[28] Georgi S Medvedev. The nonlinear heat equation on dense graphs and graph limits. *SIAM Journal on Mathematical Analysis*, 46(4):2743–2766, 2014.

[29] Hossein Mobahi, Mehrdad Farajtabar, and Peter L Bartlett. Self-distillation amplifies regularization in hilbert space. *arXiv preprint arXiv:2002.05715*, 2020.

[30] Federico Monti, Davide Boscaini, Jonathan Masci, Emanuele Rodola, Jan Svoboda, and Michael M Bronstein. Geometric deep learning on graphs and manifolds using mixture model cnns. In *CVPR*, pages 5115–5124, 2017.

[31] Galileo Namata, Ben London, Lise Getoor, Bert Huang, and UMD EDU. Query-driven active surveying for collective classification. In *International Workshop on Mining and Learning with Graphs*, 2012.

[32] Ali Rahimi, Benjamin Recht, et al. Random features for large-scale kernel machines. In *NIPS*.

[33] Adriana Romero, Nicolas Ballas, Samira Ebrahimi Kahou, Antoine Chassang, Carlo Gatta, and Yoshua Bengio. Fitnets: Hints for thin deep nets. *arXiv preprint arXiv:1412.6550*, 2014.

[34] Laurent Saloff-Coste. *Aspects of Sobolev-type inequalities*, volume 289. Cambridge University Press, 2002.

[35] Prithviraj Sen, Galileo Namata, Mustafa Bilgic, Lise Getoor, Brian Galligher, and Tina Eliassi-Rad. Collective classification in network data. *AI magazine*, 2008.

[36] Ilya Tolstikhin, Neil Houlsby, Alexander Kolesnikov, Lucas Beyer, Xiaohua Zhai, Thomas Unterthiner, Jessica Yung, Daniel Keysers, Jakob Uszkoreit, Mario Lucic, et al. Mlp-mixer: An all-mlp architecture for vision. *arXiv preprint arXiv:2105.01601*, 2021.

[37] Vladimir Vapnik, Rauf Izmailov, et al. Learning using privileged information: similarity control and knowledge transfer. *JMLR*, 16(1):2023–2049, 2015.

[38] Dmitri V Vassilevich. Heat kernel expansion: user's manual. *Physics reports*, 388(5-6):279–360, 2003.

[39] Petar Veličković, Guillem Cucurull, Arantxa Casanova, Adriana Romero, Pietro Lio, and Yoshua Bengio. Graph attention networks. *ICLR*, 2018.

[40] Shuai Wang, Kun Zhang, Le Wu, Haiping Ma, Richang Hong, and Meng Wang. Privileged graph distillation for cold start recommendation. *arXiv preprint arXiv:2105.14975*, 2021.

[41] Yifei Wang, Yisen Wang, Jiansheng Yang, and Zhouchen Lin. Dissecting the diffusion process in linear graph convolutional networks. *NeurIPS*, 2021.

[42] Andrew Gordon Wilson, Zhiting Hu, Ruslan Salakhutdinov, and Eric P Xing. Deep kernel learning. In *Artificial intelligence and statistics*, pages 370–378. PMLR, 2016.

[43] Felix Wu, Amauri Souza, Tianyi Zhang, Christopher Fifty, Tao Yu, and Kilian Weinberger. Simplifying graph convolutional networks. In *ICML*, pages 6861–6871, 2019.

[44] Shu Wu, Mengqi Zhang, Xin Jiang, Xu Ke, and Liang Wang. Personalizing graph neural networks with attention mechanism for session-based recommendation. *TKDE*, 2019.

[45] Bai Xiao, Edwin R Hancock, and Richard C Wilson. Geometric characterization and clustering of graphs using heat kernel embeddings. *Image and Vision Computing*, 28(6):1003–1021, 2010.

[46] Bencheng Yan, Chaokun Wang, Gaoyang Guo, and Yunkai Lou. Tinygnn: Learning efficient graph neural networks. In *KDD*, pages 1848–1856, 2020.

[47] Cheng Yang, Jiawei Liu, and Chuan Shi. Extract the knowledge of graph neural networks and go beyond it: An effective knowledge distillation framework. In *WWW*, pages 1227–1237, 2021.

[48] Yiding Yang, Jiayan Qiu, Mingli Song, Dacheng Tao, and Xinchao Wang. Distilling knowledge from graph convolutional networks. In *CVPR*, 2020.

[49] Junho Yim, Donggyu Joo, Jihoon Bae, and Junmo Kim. A gift from knowledge distillation: Fast optimization, network minimization and transfer learning. In *CVPR*, 2017.

[50] Sergey Zagoruyko and Nikos Komodakis. Paying more attention to attention: Improving the performance of convolutional neural networks via attention transfer. *ICLR*, 2017.

[51] Ke Zhang, Carl Yang, Xiaoxiao Li, Lichao Sun, and Siu Ming Yiu. Subgraph federated learning with missing neighbor generation. *NeurIPS*, 34, 2021.

[52] Shichang Zhang, Yozen Liu, Yizhou Sun, and Neil Shah. Graph-less neural networks: Teaching old mlps new tricks via distillation. *arXiv preprint arXiv:2110.08727*, 2021.

# Checklist

1. For all authors...
   (a) Do the main claims made in the abstract and introduction accurately reflect the paper's contributions and scope? [Yes]
   (b) Did you describe the limitations of your work? [Yes]
   (c) Did you discuss any potential negative societal impacts of your work? [Yes]
   (d) Have you read the ethics review guidelines and ensured that your paper conforms to them? [Yes]
2. If you are including theoretical results...
   (a) Did you state the full set of assumptions of all theoretical results? [Yes]
   (b) Did you include complete proofs of all theoretical results? [Yes] See Appendix A,B,C,D
3. If you ran experiments...
   (a) Did you include the code, data, and instructions needed to reproduce the main experimental results (either in the supplemental material or as a URL)? [Yes] See Appendix E for dataset information. See the supplementary for our codes
   (b) Did you specify all the training details (e.g., data splits, hyperparameters, how they were chosen)? [Yes] See Appendix E,F
   (c) Did you report error bars (e.g., with respect to the random seed after running experiments multiple times)? [Yes] See the experiment section
   (d) Did you include the total amount of compute and the type of resources used (e.g., type of GPUs, internal cluster, or cloud provider)? [Yes] See Appendix E
4. If you are using existing assets (e.g., code, data, models) or curating/releasing new assets...
   (a) If your work uses existing assets, did you cite the creators? [Yes] See Appendix E
   (b) Did you mention the license of the assets? [N/A]
   (c) Did you include any new assets either in the supplemental material or as a URL? [N/A]
   (d) Did you discuss whether and how consent was obtained from people whose data you're using/curating? [N/A]
   (e) Did you discuss whether the data you are using/curating contains personally identifiable information or offensive content? [N/A]
5. If you used crowdsourcing or conducted research with human subjects...
   (a) Did you include the full text of instructions given to participants and screenshots, if applicable? [N/A]
   (b) Did you describe any potential participant risks, with links to Institutional Review Board (IRB) approvals, if applicable? [N/A]
   (c) Did you include the estimated hourly wage paid to participants and the total amount spent on participant compensation? [N/A]